

Supernova neutrinos and the ν_τ mass.

Gianni FIORENTINI^{1,2} and Camillo ACERBI¹

¹ Istituto Nazionale di Fisica Nucleare - Sezione di Ferrara

² Dipartimento di Fisica - Università di Ferrara

12, via Paradiso – I-44100 Ferrara – ITALY

December 23, 1996

Abstract

We perform an extensive investigation of the sensitivity to non-vanishing ν_τ mass in a large water Čerenkov detector, developing an analysis method for neutrino events originated by a supernova explosion. This approach, based on directional considerations, provides informations almost undepending on the supernova model. We analyze several theoretical models from numerical simulations and phenomenological models based on *SN1987A* data, and determine optimal values of the analysis parameters so as to reach the highest sensitivity to a non-vanishing ν_τ mass. The minimal detectable mass is generally just above the cosmologically interesting range, $m \sim 100$ eV, in the case of a supernova explosion near the galactic center. For the case that no positive signal is obtained, observation of a neutrino burst with Super-Kamiokande will anyhow lower the present upper bound on ν_τ mass to few hundred eV.

1 Introduction.

Upper bounds on the electron (anti-) neutrino mass at the level of few eV are obtained from β decay experiments [1], and have been confirmed by data on neutrinos from *SN1987A*, collected by Kamiokande-II [4] and IMB [5] detectors, see e.g. [2, 3]. Concerning the masses of ν_μ and ν_τ , the present experimental bounds are much less compelling: $m_{\nu_\mu} \lesssim 170$ keV, $m \lesssim 24$ MeV [1]. Therefore, any approach capable of significantly lowering these limits is highly desirable. Particularly, an observation sensitive to neutrino masses in the range 10 – 100 eV would be extremely important for cosmological implications, see [6]. Previous analyses [7, 8] claimed that this goal might be reached with new generation larger detectors, for a supernova near the galactic center.

The questions we address in this paper are the following:

1. Which assumptions about neutrino emission are critical for observing the effects of a non-vanishing mass?
2. How the analysis procedure can be optimized in order to reach the highest sensitivity to neutrino masses?
3. Which masses for ν_μ and ν_τ can be actually explored with a detector such as Super-Kamiokande?

In general, the determination of ν -masses by means of a supernova observation is based on the comparison between the detected signal and the expected one for the case $m = 0$. A non-vanishing mass, in fact, would

reflect in an overall delay of the events number distribution, and also in a spectral distortion of the signal, due to the energy dependence of the flight-time for massive neutrinos:

$$\Delta t(\epsilon_\nu) = \frac{D}{2c} \left(\frac{mc^2}{\epsilon_\nu} \right)^2 \quad (1.1)$$

where D is the supernova distance, c is the light speed, and ϵ_ν is the neutrino energy. The greatest difficulty in applying this procedure is in the dependence on the supernova model assumed to calculate the expected signal. Moreover, when interested in ν_μ and ν_τ (hereafter we will refer to these neutrinos, and their antiparticles, as ν_i), there is an additional problem: it is impossible to isolate their signal from that of ν_e and $\bar{\nu}_e$, because all ν_i detection processes (namely neutral current reactions) are allowed for electron neutrinos too.

On the other hand, charged current interactions (only possible for ν_e and $\bar{\nu}_e$ at the energies of interest) might be used to clearly identify part of the electron neutrino signal. One can thus conceive the following strategy:

1. split, by use of a distinctive signature, the overall set of events in two classes: the first one containing only ν_e and $\bar{\nu}_e$, the second one involving all neutrino species;
2. use the first class of events to derive the expected distribution for ν_e and $\bar{\nu}_e$. In view of the strict limit on m_{ν_e} , we can treat these neutrinos as massless for our purpose (e.g. from $m_{\nu_e} \lesssim 15 \text{ eV}$ [1] and equation 1.1, we get $\Delta t \sim \mathcal{O}(1 \text{ s})$ even for the lowest detectable energies, $\epsilon_\nu \simeq 5 \text{ MeV}$, for a SN near the galactic center);
3. use this distribution to infer that of ν_μ and ν_τ , again for massless neutrinos;
4. compare the observed signal with that theoretically built in the previous step and look for mass effects. We assume that only one neutrino (say ν_τ) is massive and that flavor oscillations do not occur (see [9] and references therein for search of ν_τ mass by use of MSW effects). The comparison should be performed in the second class of events ($\nu_e + \nu_i$): in such a way we deal with a subset which still includes the whole ν_i signal, but only a part of the $\bar{\nu}_e$ “background”.

The residual dependence on the supernova model is essentially in step 3: how to connect the ν_e and $\bar{\nu}_e$ emission features with those of ν_i . In this paper we extensively investigate this point, by analyzing several theoretical and phenomenological SN models and their implications for the extraction of a non-vanishing ν_τ mass.

We also discuss how the analysis procedure can be optimized, by a proper choice of the parameters, such as energy and time windows where to look for mass effects.

Concerning the sensitivity to neutrino mass, two points are interesting: the minimal detectable ν_τ mass and the upper limit which can be established on m when no positive signal comes out. Correspondingly, we shall address the following questions:

- 3a. What is the minimal m value expected to give a signal distinguishable from the statistical fluctuations of the massless case?
- 3b. What is the minimal m value for which the signal expected for massless neutrinos can be discriminated from the statistical fluctuations of the massive case?

The paper is organized as follows: we develop a method of data analysis, based on directional considerations (Section 2) which we use to determine the minimal detectable ν_τ mass for a set of theoretical supernova models (Section 3). The same analysis is repeated for a set of phenomenological models derived from *SN1987A* data (Section 4). We then compare our results with those of ref. [10] (Section 5). Finally, we calculate, both for theoretical and phenomenological models, the mass upper bound obtainable through the same method (Section 6). Detector characteristics, cross sections and expression for event rates are collected in the Appendix.

2 The analysis method: isotropic vs. directional signal.

Krauss *et al.* [10] proposed in 1992 a beautiful procedure of data analysis for Čerenkov detectors, based on directional considerations. In this section we briefly recall the idea and then we specify our approach to this method in terms of: *i*) the kinematical characterization of neutrino events; *ii*) the assumptions needed to connect the emission features of electron and other flavors neutrinos; *iii*) the quantitative criterion for the evidence of a non-vanishing ν_τ mass.

2.1 Generalities.

Let us consider Super-Kamiokande (SK hereafter), a water Čerenkov detector whose main characteristics are listed in the Appendix, see also [11]. Neutrino events are originated basically in processes of four kinds:

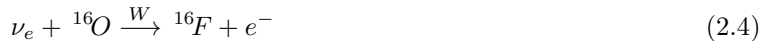
1. *capture on a proton:*



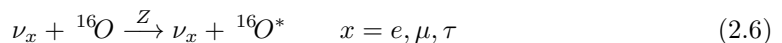
2. *scattering off an electron:*



3. *capture on an oxygen nucleus:*



4. *coherent scattering off an oxygen nucleus:*



Expressions for the cross sections are collected in the Appendix. The approximate numbers of expected events in SK, for a *SN1987A*-like supernova near the galactic center, are shown in Table 1, see also [12].

$\bar{\nu}_e p \rightarrow e^+ n$	$\simeq 5000$
$\bar{\nu}_e e^- \rightarrow \bar{\nu}_e e^-$	$\simeq 100$
$\nu_i e^- \rightarrow \nu_i e^-$	$\simeq 2 \times 25$
$\bar{\nu}_e O \rightarrow \bar{\nu}_e O$	$\simeq 50$
$\nu_x O \rightarrow \nu_x O$	$\simeq 200$ [13]

Table 1: *Expected events in SK for a supernova at galactic center.*

Among the four processes, scattering off electrons is the only directional one. For capture reactions and interactions with nuclei, the observable particles (e^\pm or γ) are emitted (almost) isotropically, whereas in processes (2.2-3) the recoil electron's angular distribution is strongly forward peaked. Therefore one can define an appropriate observation angle ϑ_{fw} , along the supernova direction, which includes all of the electrons from $\nu - e$ scattering.

Here is the required signal splitting: outside the forward cone, nearly any event is originated by ν_e and $\bar{\nu}_e$. The only contribution of other flavors neutrinos is due to (2.6), and can easily be excluded by raising the minimal

detected energy up to $7 - 8 \text{ MeV}$ [13]. So we can regard this signal as untouched by mass effects, and use it to derive the expected distribution in the forward cone for the case $m = 0$.

The analysis procedure is sketched in Figure 1.

2.2 Kinematics.

A specification of the forward observation angle ϑ_{fw} for the analysis.

When a neutrino with energy ϵ_ν scatters off an electron at rest which gets kinetic energy ϵ_e , the electron scattering angle ϑ is determined from energy-momentum conservation:

$$\cos \vartheta(\epsilon_\nu, \epsilon_e) = \sqrt{\frac{\epsilon_e}{\epsilon_e + 2m_e}} \left(1 + \frac{m_e}{\epsilon_\nu}\right) \quad (2.7)$$

As ϑ is a decreasing function of ϵ_e and a rising function of ϵ_ν , the maximum value ϑ_{max} is obtained by taking in (2.7) the minimal detected energy ϵ_{min} and taking the limit $\epsilon_\nu \rightarrow \infty$. In this way one has:

$$\vartheta_{max}(\epsilon_{min}) = \text{acos} \sqrt{\frac{\epsilon_{min}}{\epsilon_{min} + 2m_e}} \quad (2.8)$$

For the lowest value of ϵ_{min} (i.e. the energy threshold of SK, $\epsilon_{th} = 5 \text{ MeV}$) this gives $\vartheta_{max} \simeq 24^\circ$.

In Figure 2 we plot the angular distribution of the ν_τ scattered electrons along the supernova direction, for two significative values of the lower cut: $\epsilon_{min} = 5 \text{ MeV}$ (SK threshold) and $\epsilon_{min} = 15 \text{ MeV}$ (the highest value useful for the analysis, as we shall see). Although for these calculations we used the “reference” model to be described in Section 3, very similar distributions are obtained from other supernova models. In the same figure a plot of ϑ_{max} is given as a function of the lower energy cut.

Besides this purely kinematic dispersion, a systematic angular uncertainty is also present, due to the detector. This uncertainty is a decreasing function of the scattered electron energy too, for more energetic particles originate more Čerenkov light, and so one can point back to their directions with greater accuracy. The probability to detect an electron at an angle α from the scattering direction is assumed to be a gaussian function

$$dP(\alpha, \epsilon_e) \propto e^{-\frac{1}{2} \left(\frac{\alpha}{\sigma_\alpha(\epsilon_e)}\right)^2} d\alpha \quad (2.9)$$

where $\sigma_\alpha = \frac{1}{\sqrt{2}} \langle \vartheta_d^2 \rangle^{1/2}$ and $\langle \vartheta_d^2 \rangle^{1/2}$ is the empirically determined angular resolution of the detector for an electron with energy ϵ_e .

In Figure 3 one finds the the probability to detect an electron at an angle α from the original trajectory, as given by (2.9), for $\epsilon_e = 5, 15 \text{ MeV}$, and a plot of the angular resolution dependence on the electron energy for the Kamiokande-II detector [14]; a similar performance is expected for SK. In the case of a 5 MeV electron one has $\langle \vartheta_d^2 \rangle^{1/2} \simeq 38^\circ$.

Equation (2.9) tells us that one has a non-vanishing probability to detect a scattered electron just backward the supernova direction! This leads us to formulate a more reasonable definition for the forward observation cone than “the cone containing *all* $\nu + e$ scattering events”.

We verified that the model independent definition

$$\vartheta_{fw}(\epsilon_{min}) \equiv \sqrt{\vartheta_{max}^2(\epsilon_{min}) + \langle \vartheta_d^2 \rangle(\epsilon_{min})} \quad (2.10)$$

which can be read as the combination of the kinematic and detector spreads just like two independent errors, gives ϑ_{fw} values such that no more than one $\nu + e$ event is missed. For $\epsilon_{min} = 5 \text{ MeV}$ one has $\vartheta_{fw} \simeq 45^\circ$. The corresponding solid angle, $\Omega_{fw} = 2\pi [1 - \cos(\vartheta_{fw})]$, for $\epsilon_{min} = 5 \text{ MeV}$ includes a 95% of the ν_τ events, but only a 15% of the total $\bar{\nu}_e$ signal.

In Figure 4 one has the angular distribution of the tau-neutrino events, with respect to the supernova direction, considering both kinematic and detector spreads, while in Figure 5 we plotted the forward observation angle $\vartheta_{fw}(\epsilon_{min})$ as defined in (2.10).

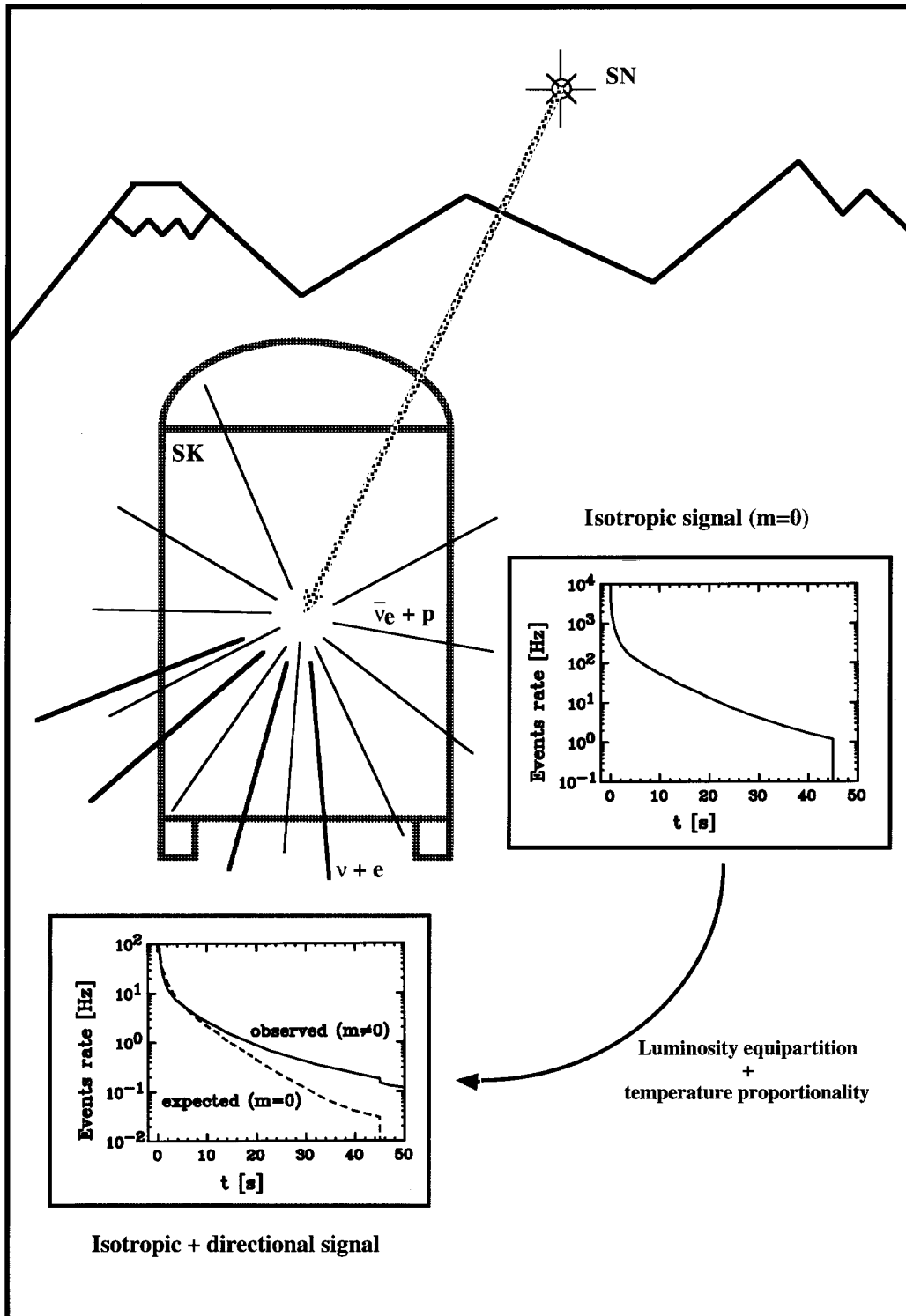


Figure 1: Sketch of the directional analysis method. Electron (anti-)neutrinos coming from the supernova originate in the detector as an isotropic signal (on the right). This one is used to infer the directional distribution for massless ν_τ (dashed line), which is to be compared with the observed signal (solid line), see bottom graph.

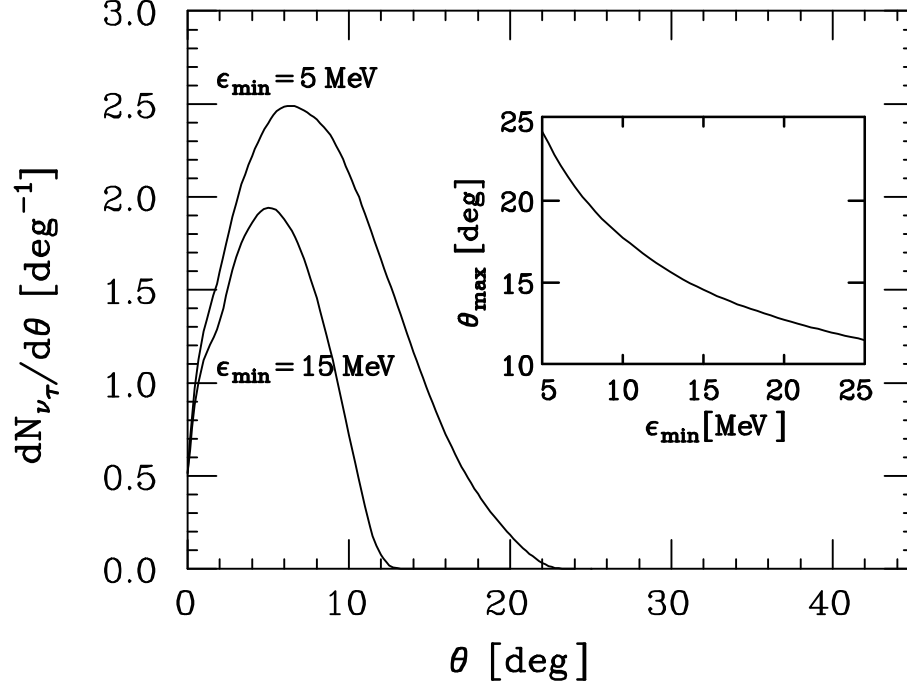


Figure 2: The angular distribution of ν_τ scattered electrons for two values of ϵ_{min} , and the maximum scattering angle ϑ_{max} as a function of the lower cut. Calculations refer to Burrows's reference model, see Section 3.1 for details.

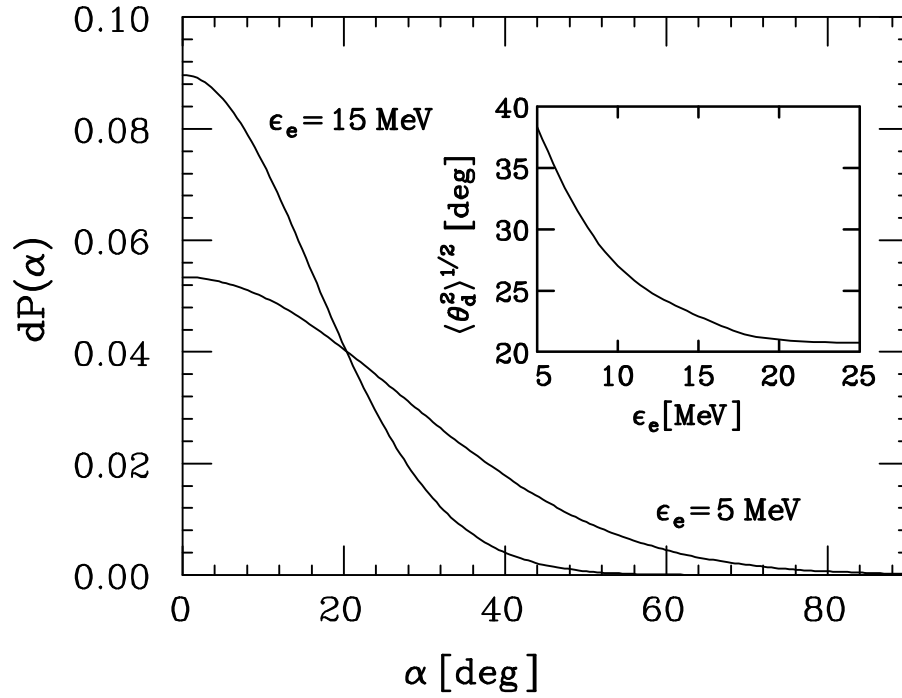


Figure 3: The probability to detect an electron at an angle α from the diffusion trajectory, for two values of ϵ_e , and the experimental angular resolution $\langle \vartheta_d^2 \rangle^{1/2}$ in Kamiokande-II, from [14].

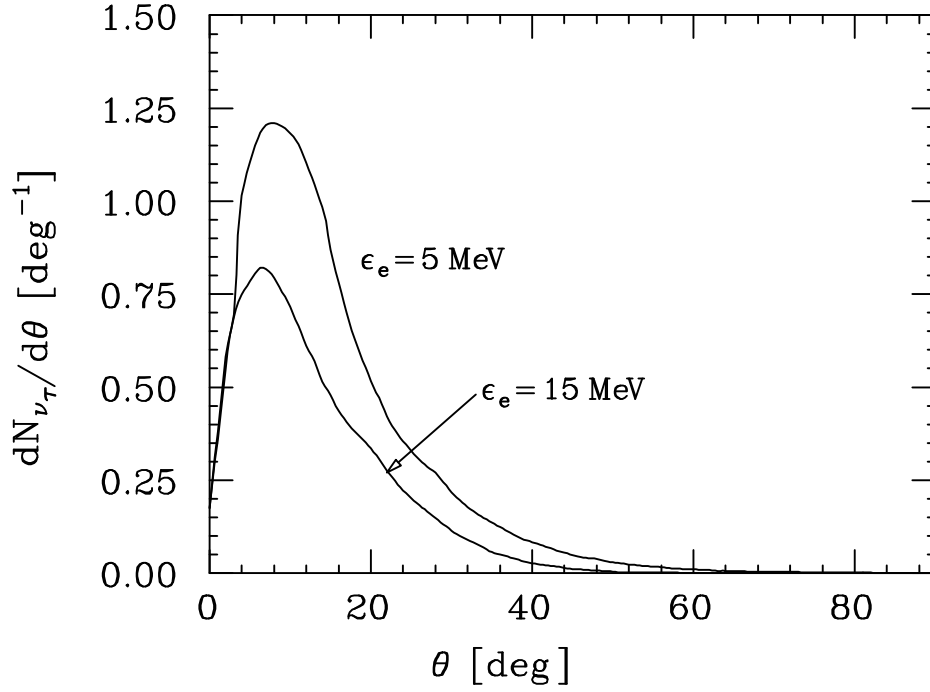


Figure 4: *The angular distribution of the $\nu_\tau + e$ signal with respect to the supernova direction, including both kinematic and detector spreads, for two significant values of ϵ_{min} . Calculations refer to Burrows's reference model (see Section 3.1).*

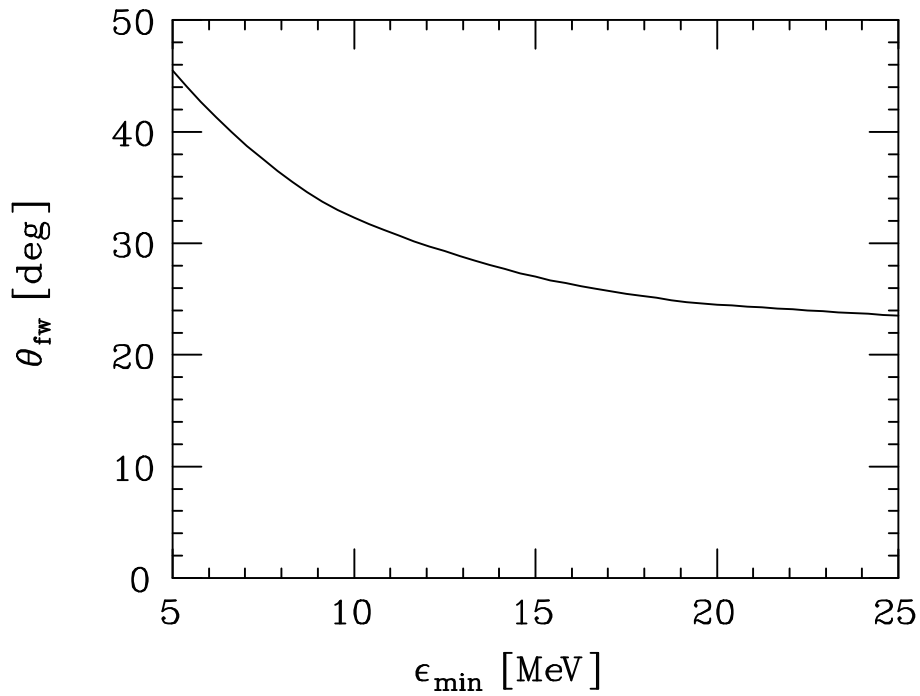


Figure 5: *The forward observation angle as a function of the lower energy cut.*

2.3 Supernova.

Next, we have to describe how the ν_i signal is derived from the $\bar{\nu}_e$ one. For this purpose, we use three assumptions, supported by the results of several numerical simulations, (see [15]) which connect the production features of electron and other flavor neutrinos *in the cooling phase*:

1. The neutrino energy distributions, at any time and for each ν species, are (approximately) thermal, thus specified by the temperatures of the neutrino-spheres $T_{\nu_e}(t)$, $T_{\bar{\nu}_e}(t)$, $T_{\nu_i}(t)$ and luminosities $L_{\nu_e}(t)$, $L_{\bar{\nu}_e}(t)$, $L_{\nu_i}(t)$. The emitted neutrino rate spectrum $d^2N_{\nu_x}/(d\epsilon_\nu dt)$ at time t and energy ϵ_ν is therefore:

$$\frac{d^2N_{\nu_x}(\epsilon_\nu, t)}{d\epsilon_\nu dt} = \frac{L_{\nu_x}(t)}{\mathcal{F}_3 T_{\nu_x}^4(t)} \frac{\epsilon_\nu^2}{1 + e^{\epsilon_\nu/T_{\nu_x}(t)}} \quad (2.11)$$

where $\mathcal{F}_3 \equiv \int_0^\infty dx x^3 (1 + e^x)^{-1} \simeq 5.68$

2. Energy equipartition among the six neutrino species holds at every time:

$$L_{\nu_e}(t) = L_{\bar{\nu}_e}(t) = L_{\nu_i}(t) \quad (2.12)$$

3. The temperatures of the six neutrino species are simply proportional at any time:

$$\begin{cases} T_{\nu_e}(t) &= \alpha_{\nu_e} \cdot T_{\bar{\nu}_e}(t) \\ T_{\nu_i}(t) &= \alpha_{\nu_i} \cdot T_{\bar{\nu}_e}(t) \end{cases} \quad (2.13)$$

Arguments supporting the second assumption can be found in [16]. Typical values of α_{ν_e} and α_{ν_i} are:

$$\begin{aligned} \alpha_{\nu_e} &= 0.5 - 0.9 \\ \alpha_{\nu_i} &= 1.1 - 1.9 \end{aligned} \quad (2.14)$$

In what follows, we fix the ratio between ν_e - and $\bar{\nu}_e$ -sphere temperatures at the central value $\alpha_{\nu_e} = 0.7$, while we'll keep α_{ν_i} as a free parameter, in the range given by (2.14).

2.4 Statistics.

Finally, we introduce our criterion to estimate the evidence level of a non-vanishing mass.

We define $N_m([t_1, t_2], [\epsilon_{min}, \epsilon_{max}])$ the expected number of events in the forward observation cone, in the time interval $[t_1, t_2]$, for an energy window $[\epsilon_{min}, \epsilon_{max}]$, if the ν_τ mass is m .

Let us assume that tau-neutrinos have mass $m \neq 0$: we expect the experiment to detect N_m events. The hypothesis that ν_τ have a vanishing mass and that the difference $|N_m - N_0|$ is due to a statistical fluctuation of the massless case can be tested by evaluating the quantity

$$s(m, [t_1, t_2], [\epsilon_{min}, \epsilon_{max}]) = \frac{|N_m - N_0|}{\sqrt{N_0}} \quad (2.15)$$

Clearly, one can vary $[t_1, t_2]$ and $[\epsilon_{min}, \epsilon_{max}]$ in order to optimize the analysis. The best indicator of a non-vanishing mass is therefore the quantity

$$S(m) = \max_{[t_1, t_2], [\epsilon_{min}, \epsilon_{max}]} \left\{ s(m, [t_1, t_2], [\epsilon_{min}, \epsilon_{max}]) \right\} \quad (2.16)$$

where the time intervals are chosen arbitrarily within the observation window (first 100 seconds after bounce), with the only request that at least an event should be present in $[t_1, t_2]$. As an example, if $S(100 \text{ eV}) = 3$ one has a 3σ evidence for a mass $m = 100 \text{ eV}$, i.e. the Confidence Level is 99.7%.

For brevity, we shall define as ‘‘detectable’’ those masses such that $S(m) \geq 3$, and we denote the minimal detectable mass as $m_{3\sigma} \equiv \min\{m : S(m) \geq 3\}$.

Note that we are using only event counts, disregarding the possible additional information of spectral deformations.

A sample of this statistical analysis is reported in Figure 6, where we plot the expected signal in the forward observation cone for $m = 0$ and $m = 200 \text{ eV}$ (for details on the model used for the calculation, see Section 3). For example, in the time interval $[t_1, t_2] = [25, 35] \text{ s}$, and for $[\epsilon_{min}, \epsilon_{max}] = [15, 25] \text{ MeV}$, one expects 1.3 events for the massless case, and 4.2 events for massive neutrinos; the evidence index is therefore $s(200 \text{ eV}, [25, 35] \text{ s}, [15, 25] \text{ MeV}) = 2.5$. We conclude that, in the time and energy intervals under examination, $m = 200 \text{ eV}$ is not sufficient to produce a clear effect.

3 Results from theoretical models of supernovæ.

Till February 1987, numerical simulations were the only way to explore supernova neutrinos features. Most of the analyses just concerned the very initial phase of the emission ($t \lesssim 1 \text{ s}$), mainly for implications on explosion mechanism, while only a few dealt with the long term cooling stage, which is relevant for us. For a review of simulations see for instance [17].

In this section we use the simulations due to Burrows [18], which describe the cooling phase, to evaluate the minimal mass m whose effects could be observed with the analysis method presented in Section 2. We also investigate the dependence of the results on the free parameters of the analysis.

3.1 Models and general results.

We performed a complete set of calculations using several supernova models taken from Burrows. In ref. [18] seventeen models are presented: disregarding “exotics” and black holes, the remaining ten models look consistent with data from *SN1987A*.

Burrows’s data, that cover the first 20 seconds for $\bar{\nu}_e$ luminosity and temperature, were extrapolated to later times by use of power-laws:

$$A(t) = A_0 \left(1 + \frac{t}{\tau_A}\right)^{-n_A}$$

where A denotes here both $L_{\bar{\nu}_e}$ and $T_{\bar{\nu}_e}$, and the parameters A_0 , τ_A and n_A are obtained from fits to late times behaviours ($t > 10 \text{ s}$). We also introduced a time parameter t_{tr} beyond which the neutrino luminosities vanish: this happens when the proto-neutron star becomes transparent to neutrinos. Typical values for t_{tr} are (40 – 50) s [12]. Finally, for the other neutrino species, luminosities and temperatures are determined through relations (2.12-13). Unless otherwise stated, all results reported in the text, tables and figures, refer to the Super-Kamiokande detector for the following “default” set of parameters:

$$\begin{aligned} \alpha_{\nu_i} &= 1.5 \\ t_{tr} &= 45 \text{ s} \\ D &= 10 \text{ kpc} \end{aligned} \tag{3.1}$$

For each model, the main characteristics are listed in Table 2, together with the results: the optimal choices for time and energy windows, and the value of the minimal detectable mass, as defined in Section 2.4. The $\bar{\nu}_e$ event rate and the sensitivity to non-vanishing neutrino mass are shown in Figures 7 and 8 for a few representative models: the *Most Favourable* case (# 52), the *Least Favourable* case (# 62) and the *REference* model (# 55), which very well accounts for *SN1987A* data.

We notice that the minimal detectable mass lies anyhow outside the cosmologically interesting region: even in the most favourable model we have $m_{3\sigma} \simeq 120 \text{ eV}$. For the reference model one has $m_{3\sigma} \simeq 140 \text{ eV}$.

When looking at the dependence on the model characteristics, we find that in general: *i*) for a given equation of state (EOS), mass effects are least pronounced for more massive cores; *ii*) for a given core mass, neutrino mass effects are weaker for the soft EOS.

Those features can be understood, at least qualitatively. We remark that, for a given EOS, the star radius decreases with mass, so that in more massive cores matter is more compressed. Also, for a given mass, softer EOS allow higher compression. Thus higher masses and/or softer EOS imply higher densities, and consequently higher temperatures and opacities. More energetic neutrinos are produced, so that ν_τ -mass induced delays are shorter. Furthermore, and more important, the longer cooling phase results in a higher background $\bar{\nu}_e$ flux at later times. The increase of the cooling time due to mass and EOS is shown in Figure 7: MF and RE models have the same EOS but different masses, whereas LF and RE models have the same mass but different EOS.

3.2 Dependence on the model parameters.

In order to investigate the dependence of the previous results on the emission parameters, we repeated our calculations by varying one parameter at a time, while keeping all the others constant at the values of (3.1). The results quoted in the following are for the reference model, but we obtained similar behaviours for the others.

We first varied the parameter α_{ν_i} , defined in Section 2.3 as the ratio of ν_{i-} to $\bar{\nu}_e$ -sphere temperatures, repeating the analysis for five different values in the range given by (2.14).

The results of this search are summarized in Table 3, where we report, for each value of the parameter, the minimal detectable mass, together with the number of ν_τ events and the characteristic delay time for $m = 150 \text{ eV}$. In Figure 9 we plot the evidence index $S(m)$ for the central value and the two extrema of the α_{ν_i} range. The minimal detectable mass depends rather weakly on the ν_i -sphere temperature. The point is that when varying α_{ν_i} two competing effects arise. For example, when α_{ν_i} is increased: *i*) the ν_τ -sphere temperature is higher, leading to more energetic neutrinos, and so to shorter delays; *ii*) the number of ν_τ events increases, leading to a higher statistics. Our calculations essentially show that these effects almost balance each other, so that small variations of α_{ν_i} do not affect substantially the sensitivity to a non-vanishing mass.

Concerning the dependence on the transparency time, we performed three calculations of the minimal detectable mass for t_{tr} around the value given by [12]. Again the results are essentially stable, see Figure 10, where we plotted the evidence index $S(m)$ for the inquired values. Clearly, the more sudden the transparency occurs, the more evident the delayed neutrinos will be: should we take the (maybe) unphysical choice $t_{tr} = 30 \text{ s}$, we find $m_{3\sigma} \simeq 110 \text{ eV}$.

Finally,....

3.3 Best choices for the analysis parameters.

These are particularly important dependences to investigate, because we deal now with detection parameters, which we can change in order to optimize the analysis.

It was already noted [10] that an upper energy cut enhances the mass sensitivity of the analysis method. This is due to the fact that the isotropic signal occurs at a higher energy with respect to the directional one. In fact in the dominant isotropic process, i.e. $\bar{\nu}_e$ capture on a proton, the emitted positron takes almost all of the neutrino energy, while in the ν_τ process, namely scattering off an electron, the average energy of the outgoing particle is roughly $\epsilon_e \sim \frac{1}{2}\epsilon_\nu$. We stress that by means of ϵ_{max} we cut high energy ν_τ events, which have short mass-induced delays, so that the loss in sensitivity is low. We should be aware, anyway, that this dynamical effect is partially balanced by the higher ν_τ energy at the emission.

Concerning the lower energy cut that we introduced, many competing effects are present, leading to a more complex situation. Basically, at high values of ϵ_{min} the number of ν_τ events get small and, most of all, we deal only with high energy neutrinos, for which the flight-time delay is shorter. On the other hand, as we said in Section 2.2, the forward observation angle is a decreasing function of the lower cut (see eq. 2.10). Rising ϵ_{min} leads therefore to a narrower cone, in which the ratio between directional and isotropic $\bar{\nu}_e$ signal becomes more favourable.

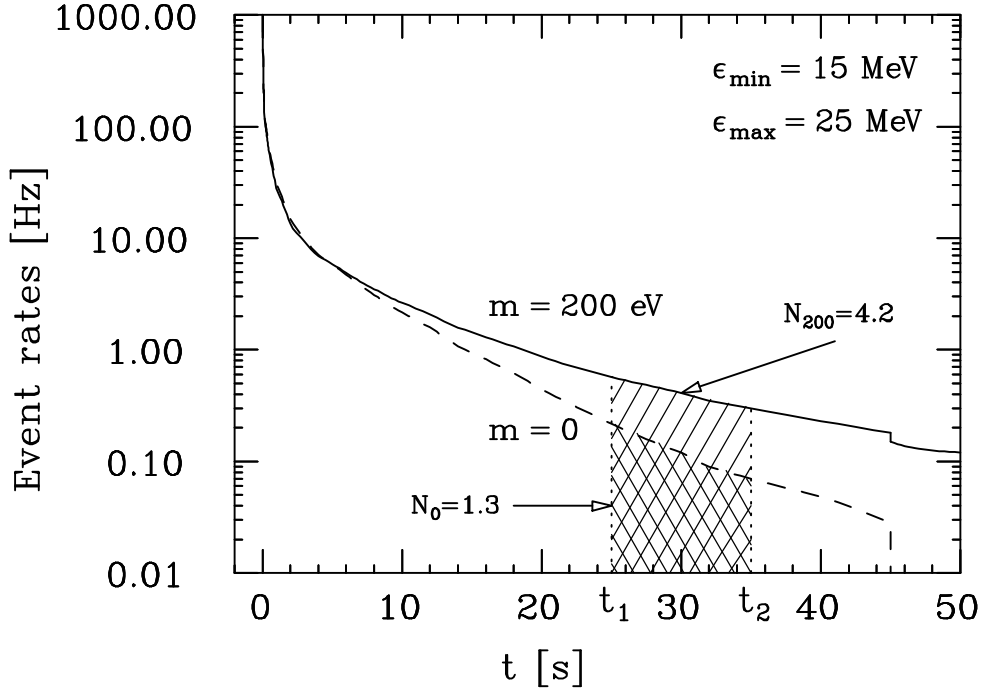


Figure 6: An example of the statistical analysis: the dashed line refers to the expected distribution in the forward observation cone for the case $m = 0$, while the solid one is for $m = 200$ eV, see text for explanations. Burrows’s “reference” model described in Section 3 was used for this example.

Model	EOS	$M_i [M_\odot]$	$M_f [M_\odot]$	$E_{tot} [foe]$	$[\epsilon_{min}, \epsilon_{max}] [MeV]$	$[t_1, t_2] [s]$	$m_{3\sigma} [eV]$
52	stiff	1.2	1.2	152	[10,20]	[25,85]	120
53	stiff	1.3	1.3	171	[10,20]	[30,95]	130
54	stiff	1.4	1.4	191	[10,20]	[30,100]	130
55	stiff	1.3	1.5	228	[10,20]	[40,95]	140
56	stiff	1.3	1.6	262	[10,20]	[45,100]	130
57	stiff	1.3	1.8	326	[10,20]	[40,95]	130
59	soft	1.2	1.2	158	[10,20]	[35,100]	140
60	soft	1.3	1.3	178	[10,20]	[40,100]	140
61	soft	1.3	1.4	205	[10,20]	[40,100]	140
62	soft	1.3	1.5	235	[10,20]	[40,100]	140

Table 2: Characteristics and results for Burrows’s supernova models: the columns indicate the equation of state (EOS), the progenitor core mass M_i , the proto-neutron star mass M_f (after accretion), the total emitted energy E_{tot} (1 foe = 10^{51} erg), the optimal energy $[\epsilon_{min}, \epsilon_{max}]$ and time $[t_1, t_2]$ windows in order to probe mass effects, and the minimal detectable mass $m_{3\sigma}$.

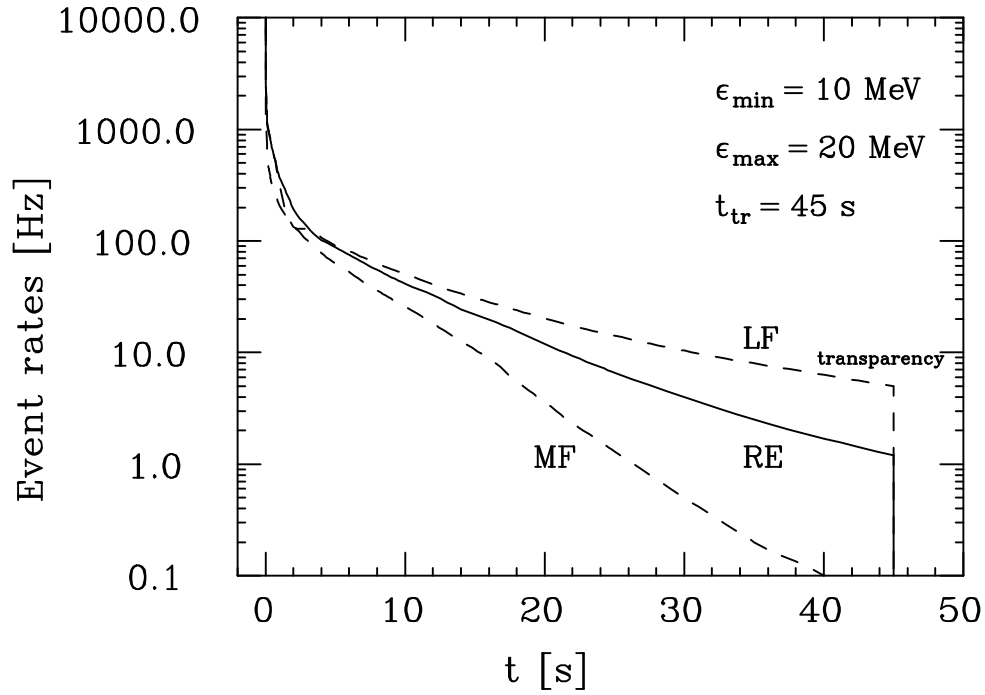


Figure 7: *The isotropic $\bar{\nu}_e$ signal in the whole SK detector, for the least/most favourable model (LF/MF), and for the “reference” model (RE), see text.*

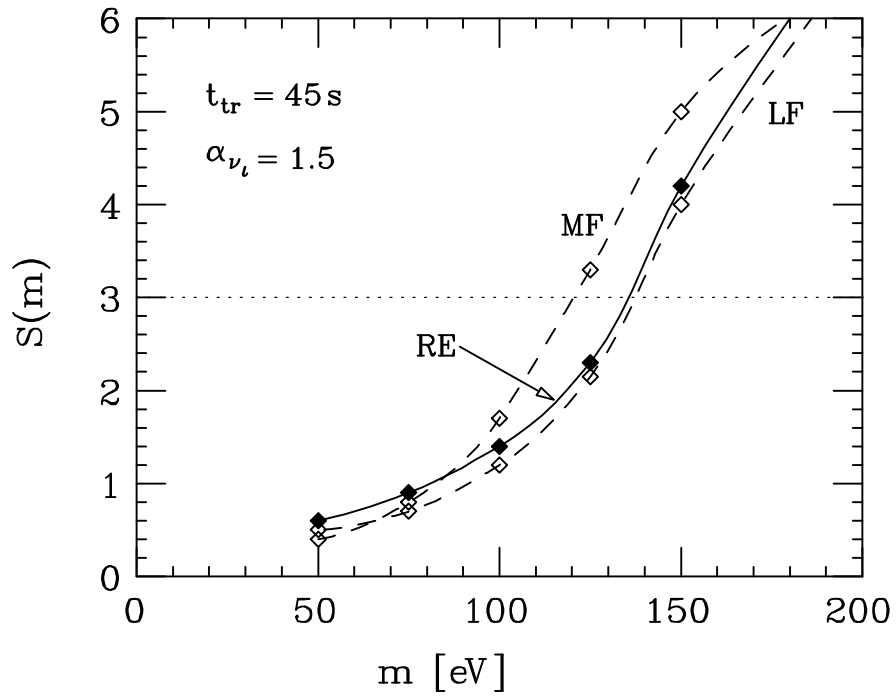


Figure 8: *Mass sensitivity for a few Burrows’s models: same notations as in Figure 7.*

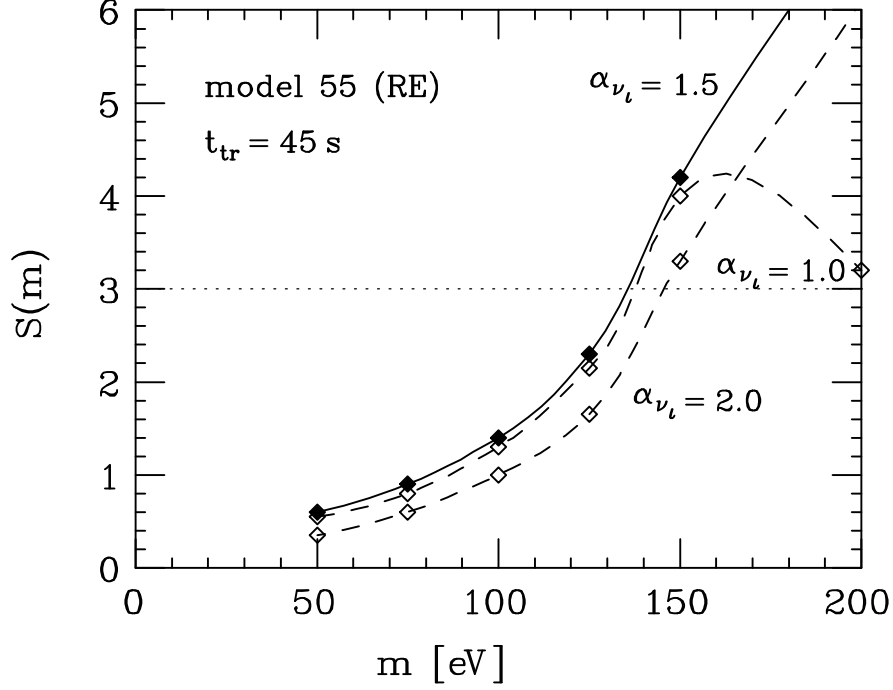


Figure 9: Mass sensitivity for several values of the ν_i -sphere temperature, in Burrows's reference model.

α_{ν_i}	N_{ν_τ}	$\Delta t(\epsilon_\nu = \alpha_{\nu_i} \cdot 15 \text{ MeV})$ [s]	$[\epsilon_{min}, \epsilon_{max}]$ [MeV]	$[t_1, t_2]$ [s]	$m_{3\sigma}$ [eV]
1.0	4.93	52	[10,20]	[35,95]	140
1.3	11.8	31	[10,20]	[35,100]	140
1.5	16.4	23	[10,20]	[40,100]	140
1.7	16.8	18	[10,20]	[40,100]	140
2.0	17.5	13	[10,20]	[40,100]	150

Table 3: Mass sensitivity dependence on the ν_i -sphere temperature in Burrows's reference model, with $t_{tr} = 45$ s. N_{ν_τ} is the number of ν_τ events in the forward cone and Δt is the characteristic delay time for a neutrino in the explorable mass range ($m = 150$ eV) and for $D = 10$ kpc.

t_{tr} [s]	$N_{\nu_\tau}(t_{tr} \rightarrow t_{max})$	$[\epsilon_{min}, \epsilon_{max}]$ [MeV]	$[t_1, t_2]$ [s]	$m_{3\sigma}$ [eV]
30	6.2	[10,20]	[30,70]	110
40	3.9	[10,20]	[35,95]	130
45	3.2	[10,20]	[40,100]	140
50	2.5	[10,20]	[40,100]	140

Table 4: Mass sensitivity dependence on the transparency time, in Burrows's reference model, with $\alpha_{\nu_i} = 1.5$. $N_{\nu_\tau}(t_{tr} \rightarrow t_{max})$ is the number of ν_τ events expected to occur after the transparency, in the case of $m = 150$ eV and for $D = 10$ kpc.

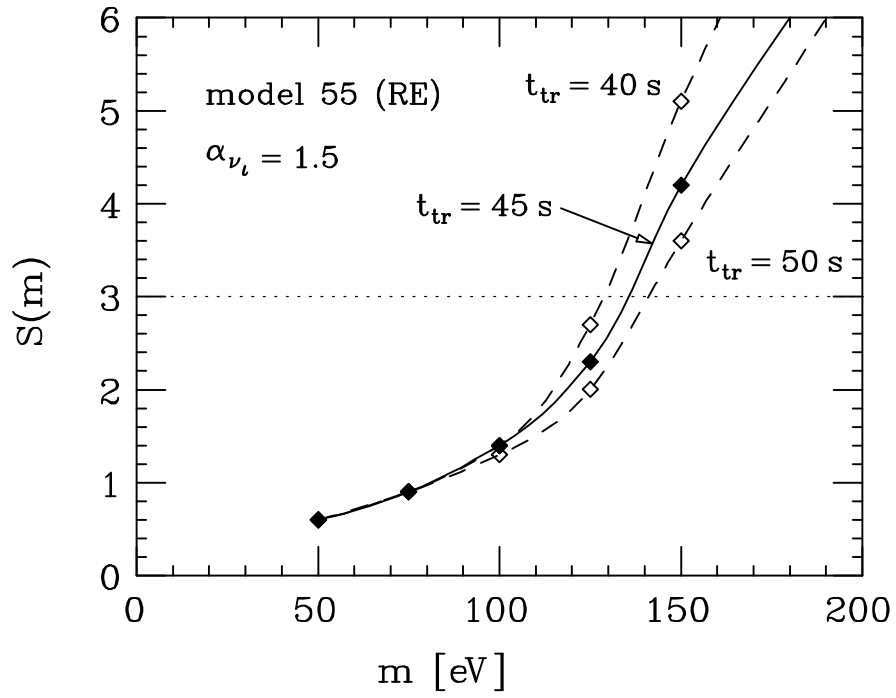


Figure 10: *Mass sensitivity for several values of the transparency time, in Burrows's reference model.*

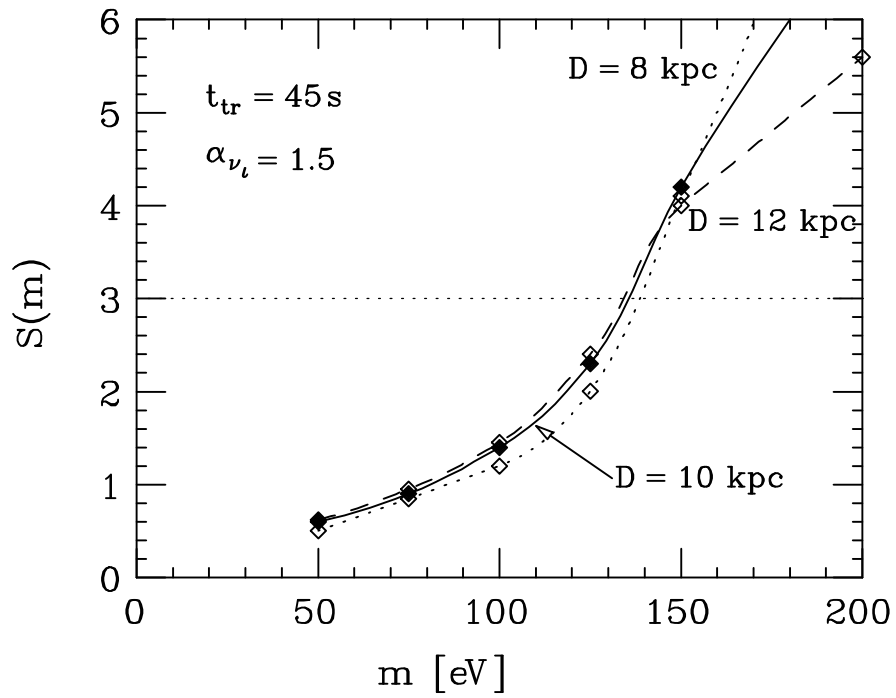


Figure 11: *Mass sensitivity for several values of the supernova distance, in Burrows's reference model.*

In Table 5 we report the full results of our analysis on the reference model for six different energy windows, while in Figure 11 we plot the mass sensitivity for three significative choices.

As we can see from Figure 11, the best choice depends on the explored mass region, because of the m dependence in the delay formula (1.1): the larger is m , the higher should be the lower cut. For our explorable range $m = 100 - 200 \text{ eV}$ the choice $\epsilon_{min} = 10 \text{ MeV}$; $\epsilon_{max} = 20 \text{ MeV}$ gives the best sensitivity for all models and for all values of the emission parameters α_{ν_i} and t_{tr} .

With regard to the time window, as we can see from Table 2 the best choice again depends on the explored mass: larger m mean more delayed neutrinos, which are to be observed at later times. For our explorable range the choice $t_1 = 40 \text{ s}$; $t_2 = 100 \text{ s}$ seems in general the most appropriate.

3.4 This section's conclusions.

We conclude, for the case of a Burrows-like supernova near the galactic center, that:

1. there is no way of getting evidence of $m \lesssim 120 \text{ eV}$;
2. this conclusion is essentially independent of the value of the uncertain emission parameters α_{ν_i} and t_{tr} ;
3. for the explorable mass range, the optimal energy window is $\epsilon_e \sim [10, 20] \text{ MeV}$.
4. for the explorable mass range, the optimal time window is $t \sim [40, 100] \text{ s}$.

4 Results from phenomenological models of supernovæ.

So far we considered theoretical models for neutrino emissions, essentially based on numerical simulations. In order to investigate further the potentialities of the analysis method, in this section we consider phenomenological models, built so as to reproduce the data from *SN1987A*.

The mere 19 events of the 1987 supernova were not sufficient to allow a detailed reconstruction of the emission features, and several models were obtained by fitting the data with different analytical functions. We selected two of these models, belonging to significative classes, to explore a wider range of possibilities.

4.1 Power-law cooling.

In this framework, we first consider a power-law parametrization, defined by the relations:

$$\begin{cases} T(t) &= T^0 \left(1 + \frac{t}{\tau}\right)^{-n} \\ L(t) &= L^0 \left(1 + \frac{t}{\tau}\right)^{-4n} \end{cases} \quad (4.1)$$

Note that, being $L(t) \propto T^4(t)$, in this model the radii of the neutrinospheres are assumed as constant.

We use as best fit parameters for *SN1987A* those obtained by Bludman & Schinder [19]:

$$\begin{cases} T_{\bar{\nu}_e}^0 &\simeq 4.20 \text{ MeV} \\ L_{\bar{\nu}_e}^0 &\simeq 19.8 \text{ foe/s} \\ \tau &\simeq 2.78 \text{ s} \\ n &\simeq 0.4 \end{cases} \quad (4.2)$$

Again we used relations (2.12-13) to derive luminosities and temperatures for the other neutrinos species.

As we can see from Figure 12, where we plotted the $\bar{\nu}_e$ event rates in SK for (4.1) and for Burrows's reference model, the behaviour of the power-law cooling is similar to that of theoretical models of Section 3.

With the values of (4.2) and for the default set of parameters (3.1), we obtained the minimal detectable mass $m_{3\sigma} \simeq 110 \text{ eV}$. This result is consistent with what found for Burrows theoretical models, and is again outside the cosmologically interesting range.

D [kpc]	N_{ν_τ}	$\Delta t(\epsilon_\nu = 20\text{MeV})$ [s]	$[\epsilon_{min}, \epsilon_{max}]$ [MeV]	$[t_1, t_2]$ [s]	$m_{3\sigma}$ [eV]
8	25.5	14.4	[10,20]	[40,100]	140
10	16.4	18.0	[10,20]	[40,100]	140
12	11.4	21.6	[10,20]	[35,100]	130
50	1.3	90.0	[5,100]	–	–

Table 5: Mass sensitivity dependence on the supernova distance, in Burrows’s reference model, with $\alpha_{\nu_i} = 1.5$ and $t_{tr} = 45$ s. N_{ν_τ} is the number of ν_τ events and Δt is the typical neutrino time-delay in the case of $m = 150$ eV.

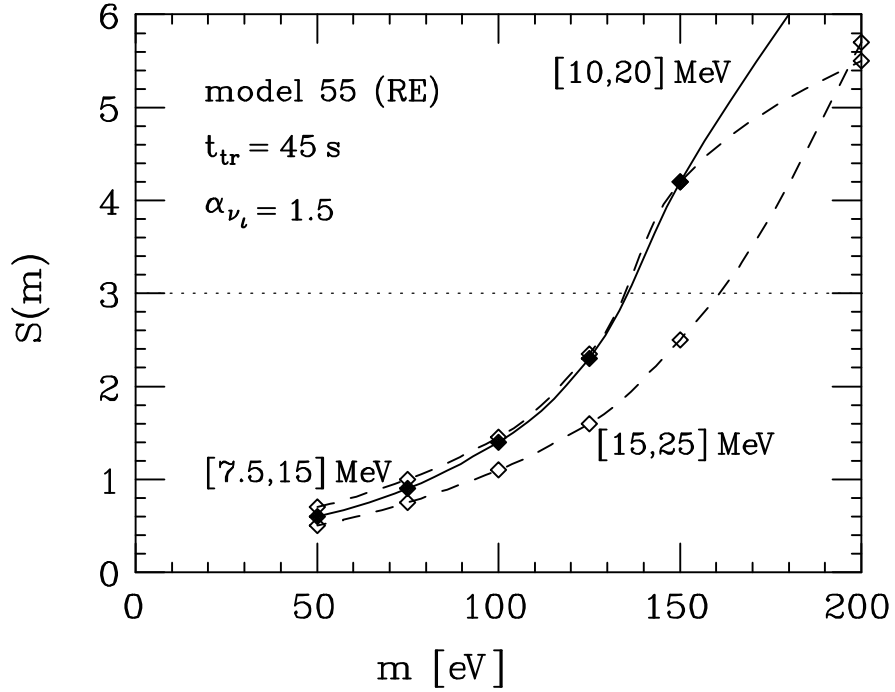


Figure 12: Mass sensitivity for significant choices of the energy window $[\epsilon_{min}, \epsilon_{max}]$, in Burrows’s reference model.

$[\epsilon_{min}, \epsilon_{max}]$ [MeV]	N_{ν_τ}/N_{tot} [%] (all SK)	ϑ_{fw} [deg]	N_{ν_τ}/N_{tot} [%] (in ϑ_{fw})	Δt_{max} [s] $\equiv \Delta t(\epsilon_\nu = \epsilon_{min})$	$[t_1, t_2]$ [s]	$m_{3\sigma}$ [eV]
[7.5, 15]	0.91	37	6.4	210	[40,100]	140
[10, 20]	0.66	32	6.5	120	[40,100]	140
[10, 100]	0.52		5.4		[30,100]	190
[15, 25]	0.48	27	7.0	52	[20,80]	160
[15, 100]	0.43		6.4		[20,90]	170
[20, 100]	0.39	24	6.8	29	[20,90]	180

Table 6: Mass sensitivity for significant energy windows, in Burrows’s reference model. Calculations are for $t_{tr} = 45$ s and $\alpha_{\nu_i} = 1.5$. Δt_{max} is the maximum delay for a neutrino in the explorable mass range ($m = 150$ eV), corresponding to the case of minimal detected energy, for $D = 10$ kpc.

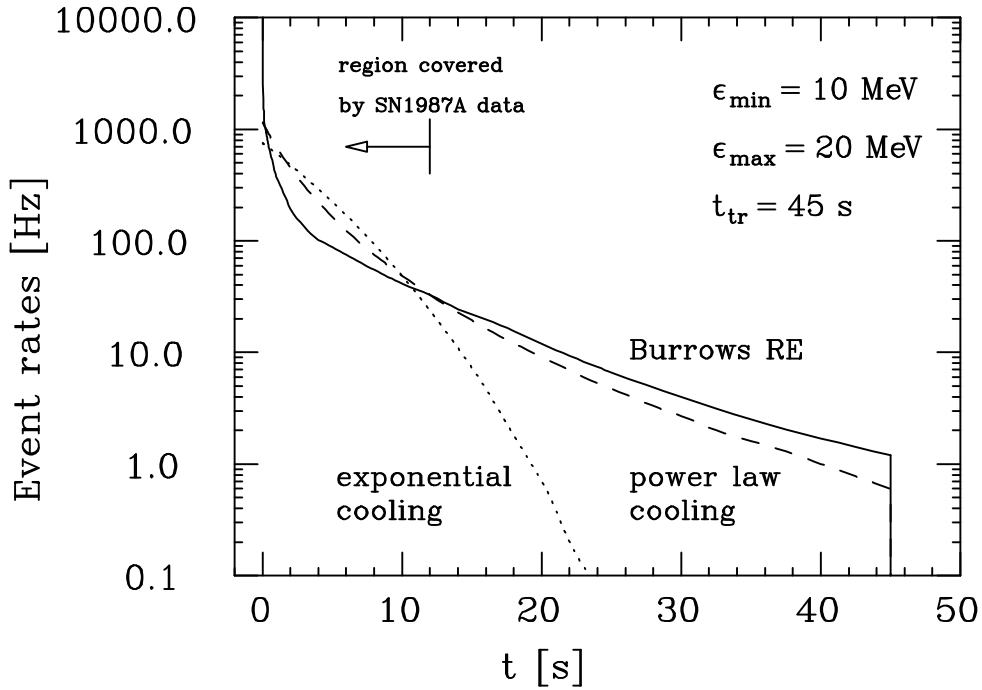


Figure 13: Total signals in the whole detector for exponential cooling (dotted), power-law cooling (dashed), and Burrows’s reference model (solid).

4.2 Exponential cooling.

A simpler analytic parametrization is obtained assuming that the neutrinosphere temperatures fall exponentially, while the radii are again kept constant. One has this way

$$\begin{cases} T(t) &= T^0 e^{-t/4\tau} \\ L(t) &= L^0 e^{-t/\tau} \end{cases} \quad (4.3)$$

The best fit parameters for *SN1987A* are taken from Loredo & Lamb [3]:

$$\begin{cases} T_{\bar{\nu}_e}^0 &\simeq 4.16 \text{ MeV} \\ L_{\bar{\nu}_e}^0 &\simeq 12.9 \text{ foe/s} \\ \tau &\simeq 4.6 \text{ s} \end{cases} \quad (4.4)$$

With these choices one obtains a minimal detectable mass $m_{3\sigma} \simeq 70 \text{ eV}$. The exponential cooling, although not clearly distinguishable from the power-law on the grounds of the *SN1987A* data, predicts at later times ($t \gtrsim 20 \text{ s}$) a substantially reduced $\bar{\nu}_e$ flux (see again Figure 12). This behaviour can account for the sensitivity to smaller masses: in fact, with a lower $\bar{\nu}_e$ background, the presence of delayed massive neutrinos is much more evident.

Actually, there is no physical reason for assuming an exponential law, and theoretical models generally predict a slower decrease of neutrino luminosity at late times¹. Furthermore, when compared with *SN1987A* data, exponential cooling models yield fits which are worse than those of power-law models [19]. In conclusion, it seems to us that exponential cooling models are not very reliable for predicting late times neutrino luminosities.

5 Comparison with Krauss’s results.

Krauss *et al.* [10], once developed their analysis method, also evaluated the minimal detectable mass. They found that a mass as small as 50 eV is detectable at 99% C.L. with Super-Kamiokande, for a medium luminosity burst from a SN at $D = 10 \text{ kpc}$.

This result is more optimistic than we found by using Burrows’s theoretical models and/or *SN1987A* phenomenological models (we recall, e.g., that for Burrows’s most favourable model one has $m_{3\sigma} = 120 \text{ eV}$ at 99.7% C.L.).

This discrepancy can’t be ascribed to the differences in the analysis procedures. We have verified that, with our approach, one obtains for the middle model of [10] (n. 17) a minimal detectable mass $m_{3\sigma} \simeq 48 \text{ eV}$.

Actually, in the supernova models of [10], after an initial accretion phase ($t \sim 0.5 \text{ s}$), the luminosities of all neutrino flavors are assumed to decay *exponentially with a very fast rate* ($\tau_L \sim 1 \text{ s}$). This results in a quite short tail of the event distribution, and so the signal of delayed ν_τ is much more evident, as we already noted for the *SN1987A* exponential model.

This feature is evident if we compare a typical model from [10] with one of those we used in the foregoing. In Figure 13, for instance, we plotted the isotropic (scaled to ϑ_{fw}) and directional event rates both in Krauss’s model 17 and in Burrows’s model 54, which give fairly the same event number. As we can see, with just $m = 100 \text{ eV}$, in Krauss’s model the directional signal outruns the isotropic “background” after a few seconds, while in Burrows’s model this occurs only at a very later times ($t > 30 \text{ s}$).

It looks to us that the fast luminosity decay assumed in [10] is not justified since: *i*) phenomenological models with exponential cooling yield longer decay times when adapted to fit *SN1987A* data, see [3, 19]; *ii*) also theoretical models predict longer decay times, see [18] and the previous discussion.

¹We remind that cooling of a degenerate gas by black-body radiation yields a power-law decrease of temperature: $T(t) = T^0 \left(1 + \frac{t}{\tau}\right)^{-1/2}$.

6 Upper bounds.

The situation may look somehow discouraging; nevertheless we should remember that the present experimental limit to ν_τ mass is tens MeV . Therefore even in the most probable case of non-observation of mass effects, we will however significantly lower this limit.

In order to obtain actual upper bounds, anyway, we have to introduce a more stringent statistical criterion than the one we used to define our “detectable” mass. With our definition of Section 2.4, in fact, we calculated the minimal value of m expected to produce a 3σ effect, checking against statistical fluctuations of the massless case. We should now take into account fluctuations of both massive and massless case.

Therefore, the new best indicator is the quantity

$$\bar{S}(m) \equiv \max_{[t_1, t_2], [\epsilon_{min}, \epsilon_{max}]} \frac{|N_m - N_0|}{\sqrt{N_m + N_0}} \quad (6.1)$$

As an example, if $\bar{S}(100 \text{ eV}) = 3$ we can claim the upper bound $m \leq 100 \text{ eV}$ at a 3σ level, i.e. with a 99.7% Confidence Level.

In practice, N_m is generally (much) larger than N_0 , so that (6.1) can be replaced to a good approximation with:

$$\bar{S}(m) \equiv \max_{[t_1, t_2], [\epsilon_{min}, \epsilon_{max}]} \frac{|N_m - N_0|}{\sqrt{N_m}} \quad (6.2)$$

This can be read very much like (2.15), i.e. assuming that neutrinos are massless, the observer will detect N_0 events (or a number close to it). Eq. (6.2) tells then how many sigma’s the result is out of the expectation for massive neutrinos.

Model	$m_{3\sigma}$ [eV]	$[\epsilon_{min}, \epsilon_{max}]$ [MeV]	$[t_1, t_2]$ [s]	$\bar{m}_{3\sigma}$ [eV]
Burrows RE	140	[15,100]	[15,100]	200
Burrows MF	120	[10,20]	[15,95]	140
Power-law	110	[10,20]	[10,85]	140
Exponential	70	[10,20]	[10,60]	90
Krauss 17	50	[10,20]	[5,15]	70

Table 7: *The minimal excludable mass for a few significative models of supernova.*

The results for two significative theoretical models (Burrow’s reference and most favourable models - see Section 3) and two phenomenological models (exponential and power-law cooling - see Section 4) are listed in Table 6. Using the same notation of Section 2.3, we define the minimal excludable mass as $\bar{m}_{3\sigma} \equiv \min\{m : \bar{S}(m) \geq 3\}$. Clearly a larger mass is required to probe an upper bound rather than a simply detectable effect, for one has $N_m > N_0 \Rightarrow \bar{S}(m) < S(m)$. Anyway, one can see that even in the case of non-observation of mass effects, we will be able to lower the present upper bound on ν_τ mass by 5 orders of magnitude!

One should be aware, anyway, that the bounds of Table 6 (and also the previous results on the minimal detectable mass) may not hold if the ν_τ mass is too large. In this case, in fact, one has a too broad event distribution, see for instance [20]. A very crude estimate of the maximum mass m_{max} explorable by delay-based analyses can be obtained by requiring that the rate of delayed ν_τ events keeps greater than the background rate. For SK one finds roughly $m_{max} \sim \mathcal{O}(10 \text{ keV})$. Our results should be read therefore as lower extrema of an excluded mass region: in the case of non-observation of mass effects one could exclude m in the window $200 \text{ eV} - 20 \text{ keV}$.

7 Conclusions.

Let us summarize the main points of this paper:

- i) We performed an extensive investigation of the sensitivity to non-vanishing ν_τ mass in a large water Čerenkov detector, developing the analysis method introduced by Krauss *et al.* [10]. As the most important point is the dependence of the results on the supernova model, we analysed several theoretical models from numerical simulations of Burrows [18] and phenomenological models based on *SN1987A* data [19, 3].
- ii) We determined optimal values of the analysis parameters (energy cuts and time window) so as to reach the highest sensitivity to a non-vanishing ν_τ mass.
- iii) Our conclusion is that the minimal detectable mass is generally just above the cosmologically interesting range, $m \sim 100$ eV, see Table 2 for details.
- iv) Differences with respect to [10], which claimed sensitivity to significantly smaller masses, are ascribed to the shorter decay time of neutrino luminosities assumed in [10], contrary to theoretical models as well to *SN1987A* phenomenological models.
- v) For the case that no positive signal is obtained, observation of a neutrino burst with SK will anyhow lower the present upper bound on ν_τ mass ($m \lesssim 24$ MeV [1]) to few hundred eV, see Table 6.

A Appendix

A.1 Super-Kamiokande characteristics.

In Table 7 we summarize the main characteristics of the Super-Kamiokande detector (the fiducial mass, the threshold energy and detection efficiency, and the background rate spectrum) as we used in our analysis.

M_{det}^\dagger	=	32 kton	
ϵ_{th}	=	5 MeV	
$\eta(\epsilon_e)$	\simeq	$\vartheta(\epsilon_e - \epsilon_{th}) \cdot \left[0.93 - e^{-(\epsilon_e / 9 \text{ MeV})^{2.5}} \right]$	[18]
$b(\epsilon)$	\simeq	$M_{det} \cdot \frac{0.082}{\sqrt{2\pi} \cdot 0.87} e^{-\frac{1}{2} \left(\frac{\epsilon - 6.2}{0.87} \right)^2} \frac{\#}{\text{MeV s}}$	elab. [3]

[†] We refer to the fiducial mass for supernova events.

Table 8: *Super Kamiokande characteristics.*

A.2 Cross sections.

1. *capture on a proton:*

$$\frac{d\sigma_{\bar{\nu}_e p}}{d\epsilon_e} = \frac{1}{4} \sigma_0 \left(\frac{\epsilon_\nu}{m_e c^2} \right)^2 (1 + 3\alpha^2)(1 + \delta_{wm}) \left(1 - \frac{Q}{\epsilon_\nu} \right) \left[\left(1 - \frac{Q}{\epsilon_\nu} \right)^2 - \left(\frac{m_e c^2}{\epsilon_\nu} \right)^2 \right]^{1/2} \cdot \delta(\epsilon_\nu - \epsilon_e - Q) \quad (\text{A.1})$$

where $\alpha \simeq -1.26$ is the axial-vector coupling constant, $Q \simeq 1.293$ MeV is the neutron-proton mass difference, $\delta_{wm} \simeq -3.3 \cdot 10^{-3}(\epsilon_\nu - Q/2)/\text{MeV}$ is the weak-magnetism correction, and

$$\sigma_0 \equiv \frac{4}{\pi} \frac{1}{(\hbar c)^4} G_F^2 (m_e c^2)^2 \simeq 1.76 \cdot 10^{-44} \text{ cm}^2$$

2. *scattering off an electron:*

$$\frac{d\sigma_{\nu_x e}}{d\epsilon_e} = \frac{1}{2} \frac{\sigma_0}{m_e c^2} \left[A_x + B_x \left(1 - \frac{\epsilon_e}{\epsilon_\nu} \right)^2 - \frac{m_e c^2 \epsilon_e}{\epsilon_\nu^2} \sqrt{A_x B_x} \right] \quad (\text{A.2})$$

where the constants A and B have values:

$$A_x = \begin{cases} \left(\frac{1}{2} + \sin^2 \theta_W \right)^2 & \simeq 0.536 & , & \nu_e \\ \sin^4 \theta_W & \simeq 0.0538 & , & \bar{\nu}_e \\ \left(-\frac{1}{2} + \sin^2 \theta_W \right)^2 & \simeq 0.0719 & , & \nu_i \\ \sin^4 \theta_W & \simeq 0.0538 & , & \bar{\nu}_i \end{cases}$$

$$B_x = \begin{cases} \sin^4 \theta_W & \simeq 0.0538 & , & \nu_e \\ \left(\frac{1}{2} + \sin^2 \theta_W \right)^2 & \simeq 0.536 & , & \bar{\nu}_e \\ \sin^4 \theta_W & \simeq 0.0538 & , & \nu_i \\ \left(-\frac{1}{2} + \sin^2 \theta_W \right)^2 & \simeq 0.0719 & , & \bar{\nu}_i \end{cases}$$

3. *capture of a ν_e on an oxygen nucleus:*

The cross section of this process can be roughly approximated to [21]

$$\frac{d\sigma_{\nu_e O}}{d\epsilon_e} \simeq 0.16 \sigma_0 \left(\frac{\epsilon_\nu - \tilde{\epsilon}}{m_e c^2} \right)^2 \theta(\epsilon_\nu - \tilde{\epsilon}) \cdot \delta(\epsilon_\nu - \tilde{\epsilon} - \epsilon_e + m_e) \quad (\text{A.3})$$

where $\tilde{\epsilon} \sim 13 \text{ MeV}$ is an effective reaction threshold.

4. *capture of a $\bar{\nu}_e$ on an oxygen nucleus:*

We use the approximation given by [10]

$$\frac{d\sigma_{\bar{\nu}_e O}}{d\epsilon_e} \simeq 0.074 \sigma_0 \left(\frac{\epsilon_\nu - \tilde{\epsilon}}{m_e c^2} \right)^2 \theta(\epsilon_\nu - \tilde{\epsilon}) \cdot \delta(\epsilon_\nu - \tilde{\epsilon} - \epsilon_e + m_e) \quad (\text{A.4})$$

where the reaction threshold is again $\tilde{\epsilon} \sim 13 \text{ MeV}$.

A.3 From emission to detection.

Being $d^2 N_{\nu_x} / d\epsilon_\nu dt'$ the rate spectrum of ν_x emitted at time t' with energy ϵ_ν , as defined in Section 2.3, the corresponding differential flux at the detector at time t is

$$\frac{d^2 \Phi_{\nu_x}(\epsilon_\nu, t)}{d\epsilon_\nu dt} = \frac{1}{4\pi D^2} \int dt' \frac{d^2 N_{\nu_x}(\epsilon_\nu, t')}{d\epsilon_\nu dt'} \cdot \delta(t - t' - \Delta t(\epsilon_\nu, m)) \quad (\text{A.5})$$

For each detection process one obtains therefore the event rate dN_b/dt as

$$\frac{dN_b(t)}{dt} = \int_{\epsilon_{min}}^{\epsilon_{max}} d\epsilon_e \eta(\epsilon_e) \int_0^\infty d\epsilon_\nu \frac{d^2 \Phi_{\nu_x}}{d\epsilon_\nu dt} n_b \frac{d\sigma_{\nu b}(\epsilon_\nu, \epsilon_e)}{d\epsilon_e} \quad (\text{A.6})$$

where $d\sigma_{\nu b}/d\epsilon_e$ is the differential cross section of the reaction under examination, n_b is the target number, and $\eta(\epsilon_e)$ is the electron/positron detection efficiency.

For the natural background one has instead the time-independent rate

$$B(\epsilon_{min}, \epsilon_{max}) = \int_{\epsilon_{min}}^{\epsilon_{max}} d\epsilon_e b(\epsilon_e) \eta(\epsilon_e) \quad (\text{A.7})$$

where $b(\epsilon_e)$ is the empirically determinated background rate spectrum.

References

- [1] Particle Data Group, *Phys. Rev. D* **54** (1996) 1 (and references therein)
- [2] W.D. Arnett and J.L. Rosner, *Phys. Rev. Lett.* **58** (1987) 1906
D.N. Spergel and J.N. Bahcall, *Phys. Lett. B* **200** (1987) 366
- [3] T.J. Loredo and D.Q. Lamb, in: Proc. 14th Texas Symp. on Relativistic Astrophysics, *Ann. N.Y. Ac. Sc.* (1988) 601
- [4] K.S. Hirata *et al.*, *Phys. Rev. Lett.* **58** (1987) 1490
- [5] R.M. Bionta *et al.*, *Phys. Rev. Lett.* **58** (1987) 1494
- [6] S.S. Gershtein and Y.B. Zeldovich, *JETP Lett.* **4** (1966) 120 [*Zh. Eksp. Teor. Fiz. Pis'ma Red.* **4** (1966) 174]
- [7] D. Seckel, G. Steigman, and T.P. Walker, *Nucl. Phys. B* **366** (1991) 233
- [8] D.B. Cline, G.M. Fuller, W.P. Hong, B. Meyer, and J. Wilson, *Phys. Rev. D* **50** (1994) 720
- [9] H. Minakata and H. Nunokawa, *Phys. Rev. D* **41** (1990) 2976
- [10] L.M. Krauss, P. Romanelli, D. Schramm, and R. Lehrer, *Nucl. Phys. B* **380** (1992) 507
- [11] For a review on SK visit the URL <http://www-sk.icrr.u-tokyo.ac.jp/>
- [12] A. Burrows, D. Klein, and R. Gandhi, *Phys. Rev. D* **45** (1992) 3361
- [13] K. Langanke, P. Vogel, and E. Kolbe, *Phys. Rev. Lett.* **76** (1996) 2629
- [14] M. Koshiba, *Phys. Report* **220** (1992) 231
- [15] R. Mayle, J.R. Wilson, and D.N. Schramm, *Astrophys. J.* **318** (1987) 288
S.W. Bruenn, *Phys. Rev. Lett.* **59** (1987) 938
- [16] T.-H. Janka, *Astropart. Phys.* **3** (1995) 377
- [17] H. Suzuki, in: *Physics and Astrophysics of Neutrinos*, eds. M. Fukugita and A. Suzuki (Springer-Verlag, Tokyo, 1994) 763
- [18] A. Burrows, *Astrophys. J.* **334** (1988) 891
- [19] S.A. Bludman and P.J. Schinder, *Astrophys. J.* **326** (1988) 265
- [20] J.M. Soares and L. Wolfenstein, *Phys. Rev D* **40** (1989) 3666
- [21] J. Arafune and M. Fukugita, *Phys. Rev. Lett.* **59** (1987) 367

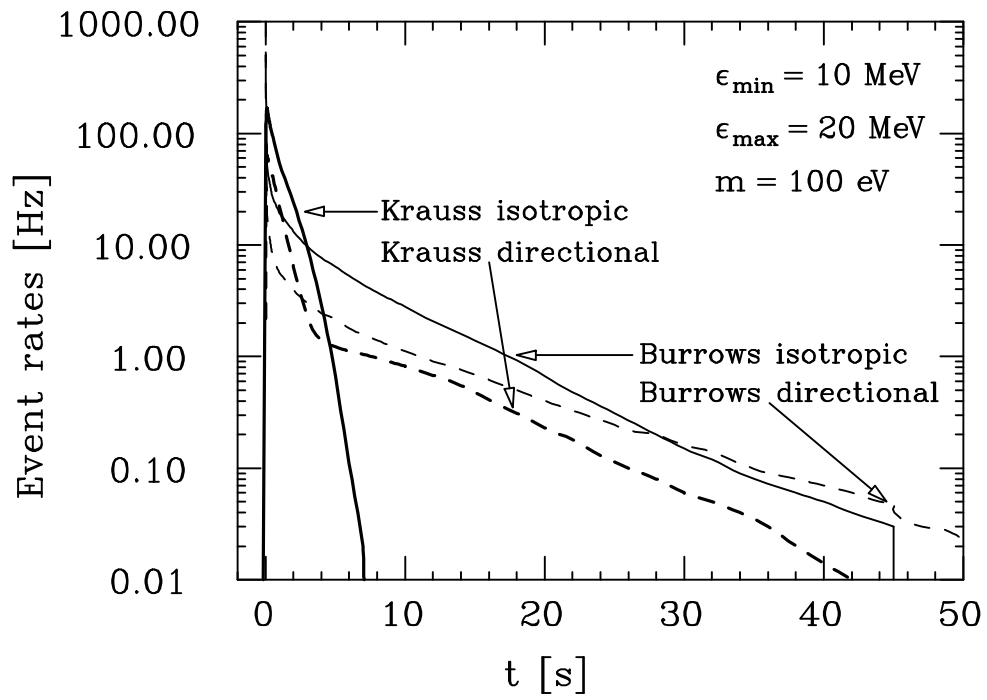


Figure 14: *Isotropic (scaled to ϑ_{fw}) and directional signals in Krauss's model n. 17 and in Burrows's model n. 54 (same event number); a $m = 100 \text{ eV}$ was assumed.*